Evidence for a Transition in the Pairing Symmetry of the Electron-Doped Cuprates $La_{2-x}Ce_xCuO_{4-y}$ and $Pr_{2-x}Ce_xCuO_{4-y}$

John A. Skinta, Mun-Seog Kim, and Thomas R. Lemberger Department of Physics, Ohio State University, Columbus, OH 43210-1106

T. Greibe and M. Naito

NTT Basic Research Laboratories, 3-1 Morinosato Wakamiya, Atsugi-shi, Kanagawa 243, Japan

(October 25, 2018)

We present measurements of the magnetic penetration depth, $\lambda^{-2}(T)$, in $\Pr_{2-x}\operatorname{Ce}_x\operatorname{CuO}_{4-y}$ and $\operatorname{La}_{2-x}\operatorname{Ce}_x\operatorname{CuO}_{4-y}$ films at three Ce doping levels, x, near optimal. Optimal and overdoped films are qualitatively and quantitatively different from underdoped films. For example, $\lambda^{-2}(0)$ decreases rapidly with underdoping but is roughly constant above optimal doping. Also, $\lambda^{-2}(T)$ at low T is exponential at optimal and overdoping but is quadratic at underdoping. In light of other studies that suggest both d- and s-wave pairing symmetry in nominally optimally doped samples, our results are evidence for a transition from d- to s-wave pairing near optimal doping.

PACS numbers: 74.25.Fy, 74.76.Bz, 74.72.Jt

A variety of experiments have demonstrated that hole-doped cuprates possess a predominantly $d_{x^2-y^2}$ gap [1,2]. In contrast, there is no consensus concerning order parameter symmetry in electron-doped cuprates. Phase-sensitive [3], angel resolved photoemission spectroscopy [4], and some penetration depth [5,6] measurements on nominally identical optimally doped $\Pr_{2-x}\text{Ce}_x\text{CuO}_{4-y}$ (PCCO) and $\text{Nd}_{2-x}\text{Ce}_x\text{CuO}_{4-y}$ (NCCO) samples suggest d-wave pairing. Other penetration depth measurements [7,8] and the absence of a zero-bias conductance peak in tunnelling measurements [9,10] indicate s-wave superconductivity.

To date, experimental studies of e-doped cuprates have concentrated on optimally doped samples. To explore the pairing symmetry controversy, we present measurements of $\lambda^{-2}(T)$ in PCCO and $\text{La}_{2-x}\text{Ce}_x\text{CuO}_{4-y}$ (LCCO) films at three dopings, x, near optimal. The curvature near T_c and the low-temperature magnitude of the superfluid density, $n_s(T) \propto \lambda^{-2}(T)$, depend strongly on doping. Furthermore, the temperature dependence of $\lambda^{-2}(T)/\lambda^{-2}(0)$ at low T changes with doping: it is exponential at optimal and overdoping, but quadratic at underdoping. These phenomena indicate some sort of transition near optimal doping. Our results here are consistent with the transition being from d- to s-wave pairing. Contradictory e-doped pairing symmetry results can thus be reconciled, if nominally optimally doped samples that exhibit d-wave properties are in reality underdoped.

Films were prepared by molecular-beam epitaxy (MBE) on 12.7 mm \times 12.7 mm \times 0.35 mm SrTiO₃ substrates as detailed elsewhere [11–13]. The same procedures and parameters were used for all films of a given compound. Table I summarizes film properties. Ce concentrations are measured by inductively coupled plasma spectroscopy and are known to better than ± 0.005 . We refer to the LCCO film with x=0.112 and the PCCO film with x=0.145 as "optimally doped", although the optimal x may be slightly smaller than these values [14]. The optimal PCCO film is film P3 from Ref. 8. The films are highly c-axis oriented, and their ab-plane resistivities, $\rho(T)$ in Fig. 1, are low. Resistivities in our e-doped films are lower than in e-doped crystals [15] and high-quality crystals of $\text{La}_{2-x}\text{Sr}_x\text{CuO}_4$ [16], the h-doped cousin of PCCO and LCCO. $\rho(T)$ in our films decreases monotonically with increasing doping, and $\rho(T)$ just above T_c decreases by a factor of two between under- and optimal doping.

We measure $\lambda^{-2}(T)$ with a low frequency two-coil mutual inductance technique described in detail elsewhere [17]. A film is centered between two small coils, and a current at about 50 kHz in one coil induces eddy currents in the film. Currents are approximately uniform through the film thickness. Data have been measured to be independent of frequency for 10 kHz $\leq f \leq 100$ kHz. Magnetic fields from the primary coil and the film are measured as a voltage across the secondary coil. We have checked that the typical excitation field (100 μ Tesla \perp to film) is too small to create vortices in the film. Because the coils are much smaller than the film, the applied field is concentrated near the film's center and demagnetizing effects at the film perimeter are irrelevant. All data presented here are in the linear response regime.

The film's sheet conductivity, $\sigma(T)d = \sigma_1(T)d - i\sigma_2(T)d$ with d the film thickness, is deduced from the measured mutual inductance. σ_1 is large enough to be detectable only near T_c . We define T_c and ΔT_c to be the temperature and full-width of the peak in σ_1 . $\lambda^{-2}(T)$ is obtained from the imaginary part of the conductivity as $\lambda^{-2}(T) \equiv \mu_0 \omega \sigma_2(T)$, where μ_0 is the magnetic permeability of vacuum. Experimental noise is typically 0.2% of $\lambda^{-2}(0)$ at low temperatures and is at least partly due to slow drift in amplifier gain. The 10% uncertainty in d is the largest source of error in

 $\lambda^{-2}(T)$. This uncertainty does not impact the temperature dependence of $\lambda^{-2}(T)/\lambda^{-2}(0)$. As the films were grown in the same MBE apparatus on successive runs, we estimate the relative uncertainty in $\lambda^{-2}(0)$ in each material to be +5%

Measurement of $\sigma_1(T)$ is a stringent test of film quality, as inhomogeneities in any layer will increase ΔT_c . Figure 2 displays $\sigma_1(T)$ measured at 50 kHz for each film. ΔT_c is typically ≤ 1 K and indicates excellent film quality. Structure in σ_1 is due to layers with slightly different T_c 's. The small peak at 19.7 K in the data from the overdoped LCCO film is probably due to a tiny bad spot at the film edge. No corresponding feature in $\lambda^{-2}(T)$ is apparent at 19.7 K (Fig. 3), indicating that this transition is unimportant to analysis of the data. T_c 's determined from resistivity (Fig. 1) and penetration depth measurements (Figs. 2 and 3) are identical.

A few more words about film quality are in order. Maximum T_c 's of e-doped films [7,8,10] are the same as or superior to those of e-doped crystals [4–6,15]. Resistivities of films are lower [15,18]. Crystals have intrinsic homogeneity problems – e.g., Ce-poor surfaces and gradients in Ce content [19,20] – as the reduction process required to remove interstitial apical oxygen can cause phase decomposition in bulk samples [11]. Optimized LCCO crystals have yet to be grown, so a comparison of LCCO films with crystals is impossible [13].

Figure 3 displays $\lambda^{-2}(T)$ for all films. The most important feature is that the evolution of $\lambda^{-2}(T)$ with doping is the same in PCCO and LCCO, despite some quantitative differences, such as the optimal values of T_c and $\lambda^{-2}(0)$ in LCCO being 20% higher and 30% lower, respectively, than in PCCO. For a given compound, $\lambda^{-2}(0)$ is about the same at optimal and overdoping, but is a factor of 2 smaller at underdoping. Upward curvature in $\lambda^{-2}(T)$ near T_c appears only at and above optimal doping. We emphasize that this feature is not due to inhomogeneity [21]. A more thorough analysis of the data [14] reveals that the upward curvature can be ascribed to the energy dependence of the density of states and is an important aspect of e-doped film behavior.

We now examine the low-temperature behavior of $\lambda^{-2}(T)$, shown in Figs. 4 and 5. We have previously found [8] that $\lambda^{-2}(T)/\lambda^{-2}(0)$ in optimally doped PCCO films is reproducibly exponential at low temperatures and obeys the equation

$$\lambda^{-2}(T) \sim \lambda^{-2}(0) \left[1 - C_{\infty} e^{-D/t} \right], \tag{1}$$

where $t \equiv T/T_c$ and $D = 0.85 = \Delta_{min}/k_BT_c$. In optimal LCCO (Fig. 5), an exponential fits $\lambda^{-2}(T)$ with a best-fit value for the minimum gap of 0.73 k_BT_c . A quadratic fit lies outside the experimental noise level and is therefore unacceptable. In overdoped PCCO and LCCO (Fig. 4), the first $\sim 5\%$ drop in $\lambda^{-2}(T)/\lambda^{-2}(0)$ also displays an exponential temperature dependence, with values of D (0.55 and 0.46, respectively) substantially smaller than at optimal doping. A best quadratic fit to overdoped PCCO data lies outside the experimental noise in places and is statistically poorer. For overdoped LCCO, the data are clearly very flat at low temperatures, and a quadratic fit is extremely poor.

In underdoped PCCO and LCCO (Fig. 5, lower curves), the first $\sim 5\%$ drop in $\lambda^{-2}(T)/\lambda^{-2}(0)$ is consistent with quadratic behavior. Lower experimental temperatures are needed to rule out an exponential dependence with a very small gap (D = 0.46 and 0.60 in underdoped PCCO and LCCO, respectively) in these films. Values of T_0 from best fits of $1 - (T/T_0)^2$ to $\lambda^{-2}(T)/\lambda^{-2}(0)$ are 20.3 K and 39.3 K for underdoped PCCO and LCCO, respectively.

The picture that emerges from the data presented here, and from data on many other films [14], is that there is some sort of transition near optimal doping. Three different features of the superfluid density – low-T magnitude, near- T_c curvature, and low-T temperature dependence – change abruptly. In our PCCO films, the changes occur over a doping range with essentially the same T_c . We note that there is an abrupt transition in the behavior of h-doped cuprates near optimal doping, which is associated with the onset of a pseudogap [22]. It may be coincidental that there are transitions in e-doped and h-doped cuprate behavior near optimal doping.

We can only speculate as to the nature of the transition. On the basis of the transition from quadratic to exponential behavior at low temperatures, we surmise that the pairing symmetry changes from d-wave to s-wave near optimal doping. This conclusion is bolstered by recent tunnelling measurements [23] that are also consistent with a d- to s-wave pairing transition near optimal doping in PCCO. There is no d-wave model that predicts flatter-than- T^2 behavior for the superfluid density at low temperatures [24–26]. We note that the picture would be clearer if the underdoped films exhibited a crossover from quadratic to linear behavior at low temperatures, as predicted for weakly disordered d-wave superconductors [24–26].

We have presented high-precision measurements of $\lambda^{-2}(T)$ in PCCO and LCCO films at various dopings near optimal. Film quality is demonstrably high. The two compounds, despite quantitative differences in T_c and other parameters, behave similarly with doping. $\lambda^{-2}(0)$ increases rapidly as optimal doping is approached from below and is roughly constant above optimal doping. Upward curvature in $\lambda^{-2}(T)$ near T_c , not associated with film inhomogeneity, develops at optimal doping and grows with overdoping. At low T, the temperature dependence of

 $\lambda^{-2}(T)$ is exponential at optimal and overdoping, but is quadratic at underdoping. Exponential behavior is consistent with a gapped state, e.g., s-wave superconductivity, while T^2 is usually associated with d-wave superconductivity. This apparent transition in pairing symmetry would reconcile contradictory literature results on e-doped cuprates, if nominally optimally doped samples that exhibit d-wave characteristics are in reality underdoped.

- [1] D.J. Van Harlingen, Rev. Mod. Phys. 67, 515 (1995).
- [2] C.C. Tsuei and J.R. Kirtley, Rev. Mod. Phys. 72, 969 (2000).
- [3] C.C. Tsuei and J.R. Kirtley, Phys. Rev. Lett. 85, 182 (2000).
- [4] N.P. Armitage et al., Phys. Rev. Lett. 86, 1126 (2001).
- [5] J.D. Kokales et al., Phys. Rev. Lett. 85, 3696 (2000).
- [6] R. Prozorov et al., Phys. Rev. Lett. 85, 3700 (2000).
- [7] L. Alff et al., Phys. Rev. Lett. 83, 2644 (1999).
- [8] J.A. Skinta et al., Phys. Rev. Lett. 88, 207003 (2002).
- [9] S. Kashiwaya et al., Phys. Rev. B 57, 8680 (1998).
- [10] L. Alff et al., Phys. Rev. B 58, 11197 (1998).
- [11] M. Naito et al., Physica (Amsterdam) **293C**, 36 (1997).
- [12] M. Naito and H. Sato, Appl. Phys. Lett. 67, 2557 (1995); H. Yamamoto et al., Phys. Rev. B 56, 2852 (1997).
- [13] M. Naito and M. Hepp, Jpn. J. Appl. Phys. Lett. 39, 485 (2000).
- [14] J.A. Skinta, M.-S. Kim, T.R. Lemberger, T. Greibe, and M. Naito, to be published.
- [15] J.D. Kokales et al., Physica (Amsterdam) 341-348C, 1655 (2000).
- [16] Y. Ando, A.N. Lavrov, S. Komiya, K. Segawa, and X.F. Sun, Phys. Rev. Lett. 87, 017001 (2001).
- [17] S.J. Turneaure et al., J. Appl. Phys. 79, 4221 (1996); S.J. Turneaure et al., ibid. 83, 4334 (1998).
- [18] P. Fournier et al., Phys. Rev. Lett. 81, 4720 (1998).
- [19] A.R. Drews et al., Physica (Amsterdam) **200C**, 122 (1992).
- [20] E.F. Skelton *et al.*, Science **263**, 1416 (1994).
- [21] We have observed upward curvature in λ^{-2} near T_c before, but never at temperatures below the fluctuation peak in σ_1 . We ascribe upward curvature with non-zero σ_1 to film inhomogeneity.
- [22] T. Timusk and B. Statt, Rep. Prog. Phys. 62, 61 (1999).
- [23] A. Biswas, P. Fournier, M.M. Qazilbash, et al., to appear in Phys. Rev. Lett.
- [24] J.F. Annett et al., in *Physical Properties of High Temperature Superconductors II*, edited by D.M. Ginsberg (World Scientific, Singapore, 1990).
- [25] P.J. Hirschfeld and N. Goldenfeld, Phys. Rev. B 48, 4219 (1993).
- [26] I. Kosztin and A.J. Leggett, Phys. Rev. Lett. **79**, 135 (1997).

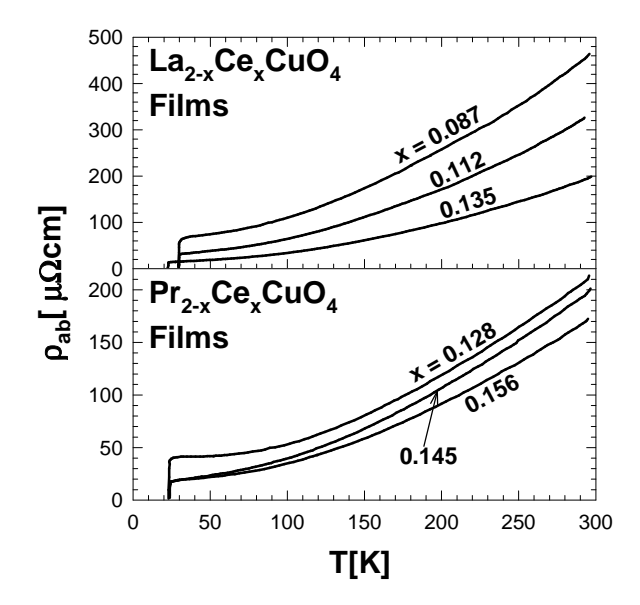


FIG. 1. ab-plane resistivities, $\rho(T)$, of six electron-doped films. For resistivities just above T_c , see Table I.

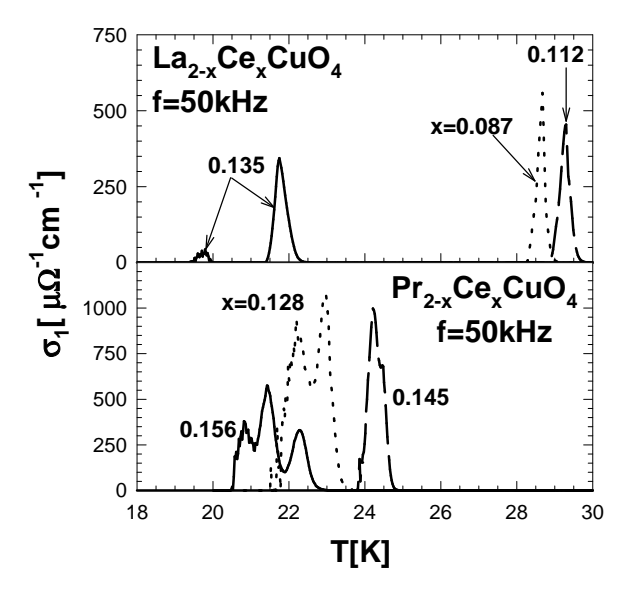


FIG. 2. $\sigma_1(T)$ at 50 kHz in six electron-doped films. T_c and ΔT_c are temperature and full-width of peak in σ_1 .

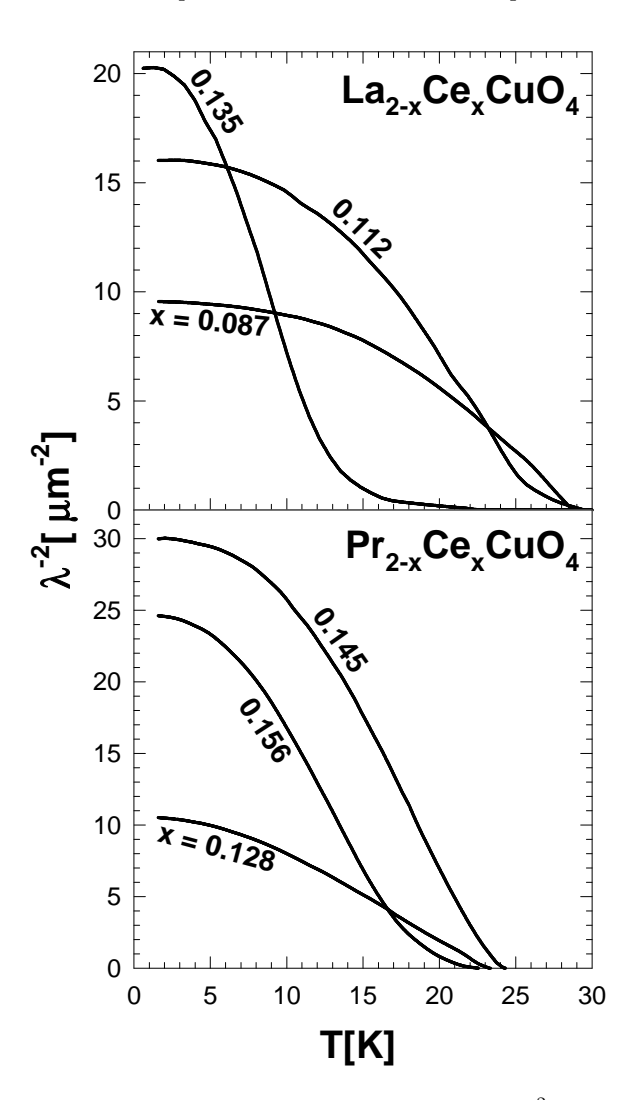


FIG. 3. $\lambda^{-2}(T)$ for six electron-doped films. Relative uncertainty in $\lambda^{-2}(0)$ in each material is $\sim 10\%$.

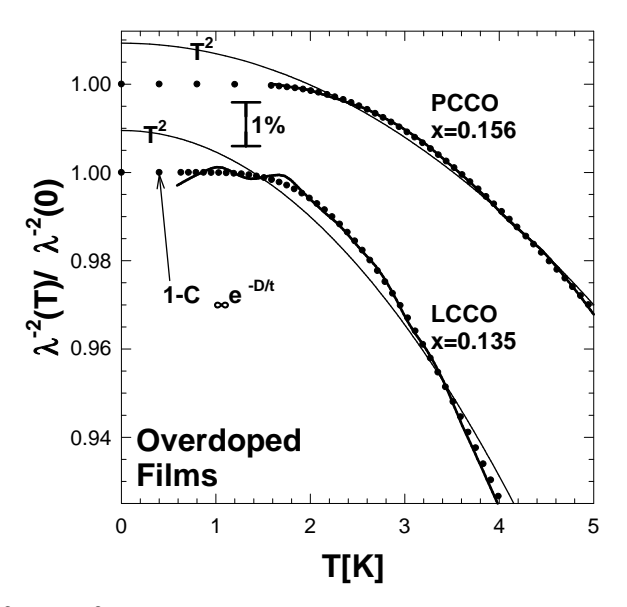


FIG. 4. First $\sim 5\%$ drop in $\lambda^{-2}(T)/\lambda^{-2}(0)$ for overdoped PCCO and LCCO films (thick lines), offset for clarity. Dotted curves are exponential fits, $1-C_{\infty}e^{-D/t}$ with $t\equiv T/T_c$, to the data over this range. Thin solid lines are best quadratic fits of the form $1-(T/T_0)^2$. Exponential fits are visibly superior.

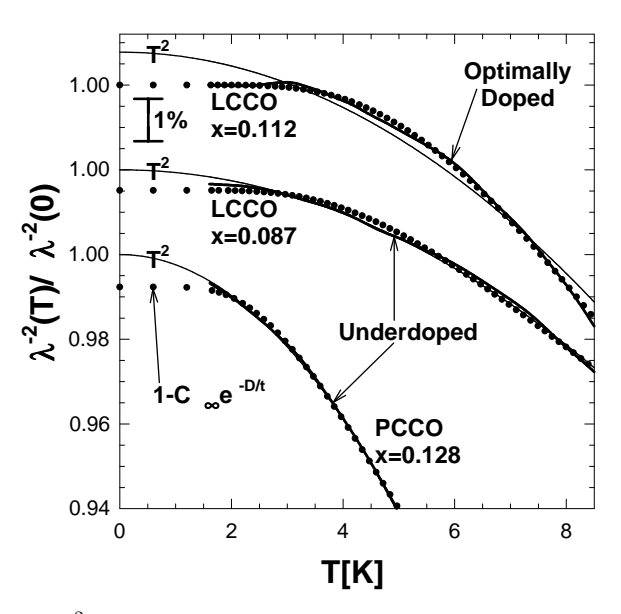


FIG. 5. First $\sim 5\%$ drop in $\lambda^{-2}(T)/\lambda^{-2}(0)$ for optimally doped (upper curve) and underdoped (lower curves) electron-doped films, offset for clarity. Dotted curves are exponential fits, $1-C_{\infty}e^{-D/t}$ with $t\equiv T/T_c$, to the data over this range. Thin solid lines are best quadratic fits of the form $1-(T/T_0)^2$. Optimally doped LCCO is exponential, and the underdoped films are quadratic, at low temperatures.

TABLE I. Properties of six electron-doped films. Ce doping, x, is measured by inductively coupled plasma spectroscopy and is known to better than ± 0.005 . d is film thickness. T_c and ΔT_c are location and full-width of peak in σ_1 . Absolute uncertainty in $\lambda^{-2}(0)$ is $\pm 10\%$. $\rho(T_c + 5K)$ is the ab-plane resistivity just above T_c . C_{∞} and D are parameters of the exponential fit in Eq. (1).

Film	x	d [Å]	T_c [K]	$\Delta T_c [K]$	$\lambda(0)$ [Å]	$\rho(T_c + 5K) \ [\mu\Omega \ \mathrm{cm}]$	C_{∞}	D
underdoped LCCO	0.087	1250	28.7	0.8	3200	67	0.32	0.60
optimal LCCO	0.112	1250	29.3	0.9	2500	33	0.69	0.73
overdoped LCCO	0.135	1250	21.7	1.0	2200	15	0.92	0.46
underdoped PCCO	0.128	1000	22.5	1.8	3100	40	0.41	0.46
optimal PCCO	0.145	1000	24.2	1.0	1800	19	0.93	0.85
overdoped PCCO	0.156	1000	21.5	2.4	2000	18	0.55	0.55